Applied Surface Science 603 (2022) 154323

Contents lists available at ScienceDirect

Applied Surface Science

journal homepage: www.elsevier.com/locate/apsusc

Full length article

Hydrogen dissociation in Li-decorated borophene and borophene hydride: An ab-initio study

Parsa Habibi [a,b], Tijin H.G. Saji [b], Thijs J.H. Vlugt [a], Othonas A. Moultos [a], Poulumi Dey [b,*]

[a] Engineering Thermodynamics, Process & Energy Department, Faculty of Mechanical, Maritime and Materials Engineering, Delft University of Technology, Leeghwaterstraat 39, Delft, 2628 CB, The Netherlands

[b] Department of Materials Science and Engineering, Faculty of Mechanical, Maritime and Materials Engineering, Delft University of Technology, Mekelweg 2, Delft, 2628 CD, The Netherlands

ARTICLE INFO

Keywords:
Hydrogen storage
Borophene hydride
Chemisorption
Hydrogen binding energy
Density functional theory
Metal decoration

ABSTRACT

Lithium (Li) dopants have garnered attention as a means to enhance hydrogen (H_2) binding energies and capacities in 2D boron-based materials. However, it is unclear if and how these dopants affect H_2 dissociation and chemisorption. Using density functional theory (DFT) and nudged elastic band (NEB) calculations, reaction pathways for H_2 dissociation on borophene-hydride and striped-borophene are investigated in the presence of Li dopants. Our results indicate that tuning the Li-loading can increase the reversibility and the rate of dehydrogenation for both borophene-hydride and striped borophene. In particular, for Li-doped borophene-hydride, the heat of reaction for H_2 release is reduced by more than 85% compared to the pristine structure (1.97 eV/H_2). Our results signify that Li-doping can considerably change the H_2 chemisorption properties of striped-borophene and borophene-hydride, and can lead to promising materials for H_2 storage.

1. Introduction

Hydrogen (H_2) molecules can be stored in materials via weak electrostatic interaction (physisorption), or by forming covalent interactions (chemisorption) [1–5]. Chemisorption of H_2 can lead to high volumetric capacities, but suffers from slow kinetics due to large energy barriers that have to be overcome to build/break H_2 bonds [6–12]. The hydrogenation reaction in chemisorption based materials, such as in metal hydrides, is usually a highly exothermic reaction [13–15]. Insufficient cooling can lead to high temperatures at which materials can degrade (e.g. sintering in metal hydrides), resulting in a lower H_2 capacity [13]. For these reasons, it is important to design materials in which the hydrogenation (dehydrogenation) reaction can occur reversibly, with little to no heat release (uptake), and with low energy barriers [6].

Two-dimensional (2D) materials are suitable for both chemisorption or physisorption alike. The large surface to volume ratio of these materials provides a large number of adsorption sites, which helps in reaching high H_2 capacities [16,17]. The electronic properties of these materials and their interaction with H_2 can also be tuned in various ways such as strain-engineering [18–20], addition of dopants [16, 21–24], vacancy creation [8,25], or by inducing charge, [26,27] or curvature [28,29]. The tuning of these electronic properties can assist in enhancing the adsorption/desorption kinetics, or the H_2 capacity. Galvanized by the synthesis of borophene (2D boron-sheets) by molecular epitaxy, the field of 2D boron-based materials has rapidly expanded [30–32]. The elaborate chemistry of boron allows for many different structural allotropes [33], anisotropic mechanical properties, electrical conductivity and favorable affinity with metal dopants [34, 35]. Borophene-hydride (also referred to as 2D hydrogen boride), which has been recently synthesized by a more facile route of cation-exchange and exfoliation [36,37], shares many of these interesting physical and chemical properties [38–40]. Due to the favorable affinity of 2D boron-based materials with metal dopants, the addition of metal decorating atoms has been a prominent method for enhancing the interaction and capacity of H_2 for physisorption storage [16,41–43]. Li dopants have been extensively considered for this application, due to their large adsorption energy with 2D boron-based materials and the low atomic mass of Li, which allows for reaching high H_2 gravimetric densities. Remarkable gravimetric densities in the range of 7–12 wt% have been reported for Li-doped borophene and borophene-hydride for H_2 physisorption-based storage [21,41,43,44]. The structural stability (including the phonon spectrum) and physical properties of various borophene-hydride and borophene structures are discussed in previous studies [39,45–47].

* Corresponding author.
E-mail address: P.dey@tudelft.nl (P. Dey).

https://doi.org/10.1016/j.apsusc.2022.154323
Received 17 May 2022; Received in revised form 14 July 2022; Accepted 18 July 2022
Available online 22 July 2022

Prior studies with borophene-hydride have shown that the addition of charge (by doping or applying a current) to the structure can destabilize the 3 center 2 electron B-H-B bonds [48,49]. As metal decorating atoms lose part of their electronic charge density to the borophene-hydride structure [41], a similar effect on the B-H-B bond may be observed. In other studies, Li has been used at high loadings on borophene-hydride and borophene structures for Li-anode batteries [38,40,50] and for H_2 physisorptive storage applications [21,41]. Despite these existing works, the influence of Li dopants on H_2 chemisorption is not apparent in Density Functional Theory (DFT), or in time-scales accessible by quantum molecular dynamics methods (order of 10 ps), even though it may be present in time scales relevant experimentally. To the best of our knowledge, the influence of Li dopants on the reversibility and activation energy barriers associated with H_2 chemisorption and dissociation has not yet been studied for borophene-hydride and striped borophene. In particular borophene-hydride could serve as a suitable H_2 storage medium, as the structure has ca. 8.5 wt % H-atoms [37], provided that the chemisorbed H-atoms can recombine with little heat uptake (reversibly) and low energy barriers (preferably below 1.5 eV [8,51]).

In this work, the H_2 chemisorption and dehydrogenation reaction pathways for Li-doped borophene-hydride and striped borophene are investigated by DFT calculations and the Nudged Elastic Band (NEB) method. It is shown that for the pristine borophene-hydride and striped borophene structures, dehydrogenation reaction is highly endothermic, exceeding 1.5 eV/H_2, and has large energy barriers (i.e., exceeding 2.0 eV). Li-dopants are shown to significantly reduce the relative energy difference between the chemisorbed and physisorbed state, thereby leading to more reversible hydrogenation/dehydrogenation reactions. The Born–Oppenheimer molecular dynamics (BOMD) simulations at 300 K show that the 3-center-2-electron bond in borophene-hydride weakens in the presence of Li dopants. The dehydrogenation energy barriers for H_2 formation are reduced by over 30% for Li doped striped-borophene and borophene-hydride. In the case of Li doped borophene-hydride, a reversible dehydrogenation reaction has been observed with low desorption/adsorption barriers. This suggests the suitability of this material for H_2 chemisorptive storage. Our findings strongly encourage further experimental study on Li-doped 2D boron-based materials to elucidate their influence on dehydrogenation/hydrogenation.

2. Computational details

2.1. Density Functional Theory (DFT)

DFT calculations are carried out using plane wave basis sets, as implemented in Vienna *ab-initio* simulation package (VASP 5.3.5).[52,53] The projected augmented wave method (PAW) is used and the generalized gradient approximation (GGA) is applied with the Perdew–Burke–Ernzerhof (PBE) exchange–correlation functional [54]. A dispersion corrected framework (DFT-D2) [55] is used. The DFT-D2 approach is commonly used in other studies of H_2 storage on 2D metal-decorated substrates [17,41–43,56]. The more recent DFT-D3 approach [57], accounts for the variations in the local environment of the atoms by considering the coordination number of each atom. Table S1 in the Supplementary Information shows a comparison between the heats of dehydrogenation computed using the DFT-D2 and DFT-D3 methods. An inter-layer separation of more than 20 Å is used, to prohibit inter-layer interactions similar to other studies on 2D substrates [41,43]. The cut-off energy is set to 550 eV for the plane-wave basis set and a Gamma-centered Monkhorst–Pack *k*-point mesh of $4 \times 4 \times 1$ is used for the structural relaxations and adsorption energy calculations. The convergence test for the *k*-point mesh is shown in Figure S1 of the Supplementary Information. The energy convergence criteria for the self-consistent electronic loop is set to 10^{-6} eV. All lattice parameters and atomic positions are relaxed until the residual forces acting on each atom are below 1 meV/Å. Gaussian smearing with a sigma of 0.05 eV is used for Brillouin-zone integration. A 3×4 conventional unit cell of borophene-hydride, containing 48 B atoms and 48 H atoms, and a 3×6 conventional supercell of striped borophene, containing 36 B atoms, are used for the DFT simulations. The choice of the system sizes is justified in tables S2 and S3 of the Supplementary Information. The system size is chosen to limit interactions between periodic images, while ensuring that the computations do not become too expensive. For a single Li-decorated borophene hydride and striped borophene structure, spin-polarized calculations are used, which converged to their non-magnetic counterparts. As both systems are found to be non-magnetic, spin-polarized calculations are not further considered for the rest of the systems studied. The Bader charges are calculated using the algorithm developed by Henkelman et al. [58–61].

2.2. Nudged Elastic Band (NEB) method

To obtain the energy barrier for formation or dissociation of H_2, the minimum energy path (MEP) is computed using the NEB method, as implemented in VASP (5.3.5) [52,53,62,63]. The energies and structures of the initial (chemisorbed) and final (physisorbed) states are calculated using DFT calculations. For the cases where the physisorbed and chemisorbed states are separated by a single transition state (no stationary states present along the reaction pathway), 5 different images are used to sample the MEP. In cases where stationary states are present in between the physisorbed and chemisorbed states, the NEB calculation is broken down into multiple segments with 5 different images connecting each stationary state. The climbing image method is used to drive the image with the highest energy towards the saddle point [64]. The same cut-off energy and *k*-point mesh is used for the NEB calculations as for the DFT calculations. For each image, all lattice parameters and atomic positions are relaxed until the residual forces acting on each atom are below 10 meV/Å.

2.3. Born–Oppenheimer Molecular Dynamics (BOMD)

To investigate finite-temperature (at 300 K) stability of borophene-hydride (with and without Li-dopants), BOMD simulations are carried out using VASP (5.3.5) [52,53]. The simulations include only the Γ-point, and are performed in the canonical ensemble (NVT). The same cut-off energy and smearing as in the DFT calculations are used. The BOMD simulations are carried out with a time-step of 1 fs. In all simulations, an initial equilibration period of 2 ps is performed, in which the temperature is increased from 0 K to 300 K. This is followed by a 10 ps production run. The variation of free energy (as defined by Kresse et al. [52]) and temperature for the BOMD simulations, as a function of simulation time is shown in Figure S2 of the Supplementary Information. A Nosé–Hoover thermostat is used [65,66]. The choice for the Nosé–Hoover mass parameter is explained in Figure S2 of the Supplementary Information. For the initial structures, the relaxed (using DFT) borophene-hydride structures (with and without Li dopants) are used. The Verlet algorithm is used for integrating the equations of motion [67]. iRASPA is used for all atomic visualizations [68].

3. Results and discussion

3.1. Borophene-hydride and striped borophene structures

The pristine borophene-hydride and striped borophene structures are shown in Fig. 1. Borophene-hydride is a planar structure with a unit cell with dimensions of 3.04 Å by 3.04 Å. For this structure the B-H, B-B (with H at bridge site), and B-B (without H at bridge site) bonds have lengths of 1.33, 1.82, and 1.72 Å, respectively. For striped borophene, a corrugated structure with a conventional/unit cell of 2.86 Å by 1.61 Å is obtained. The corrugation height of the striped borophene structure corresponds to 0.89 Å. Our structural results show a great agreement with other DFT and experimental findings for both structures [30,37,41,43].

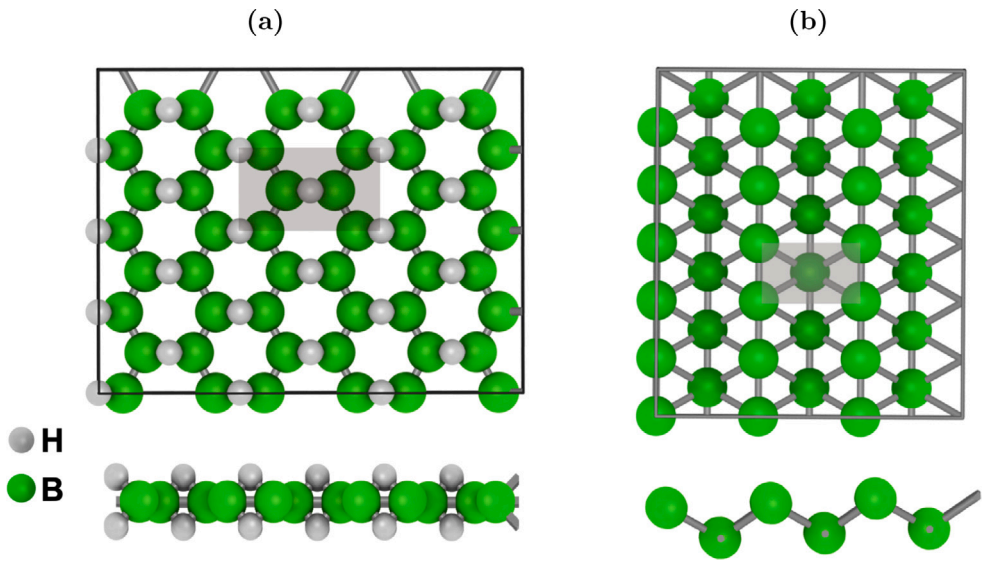

Fig. 1. Top and side views of relaxed (a) borophene-hydride with a conventional cell of 5.29 Å by 3.01 Å, and (b) striped Borophene with a conventional/unit cell of 2.86 Å by 1.61 Å. The conventional cells are indicated by a gray area for both structures.

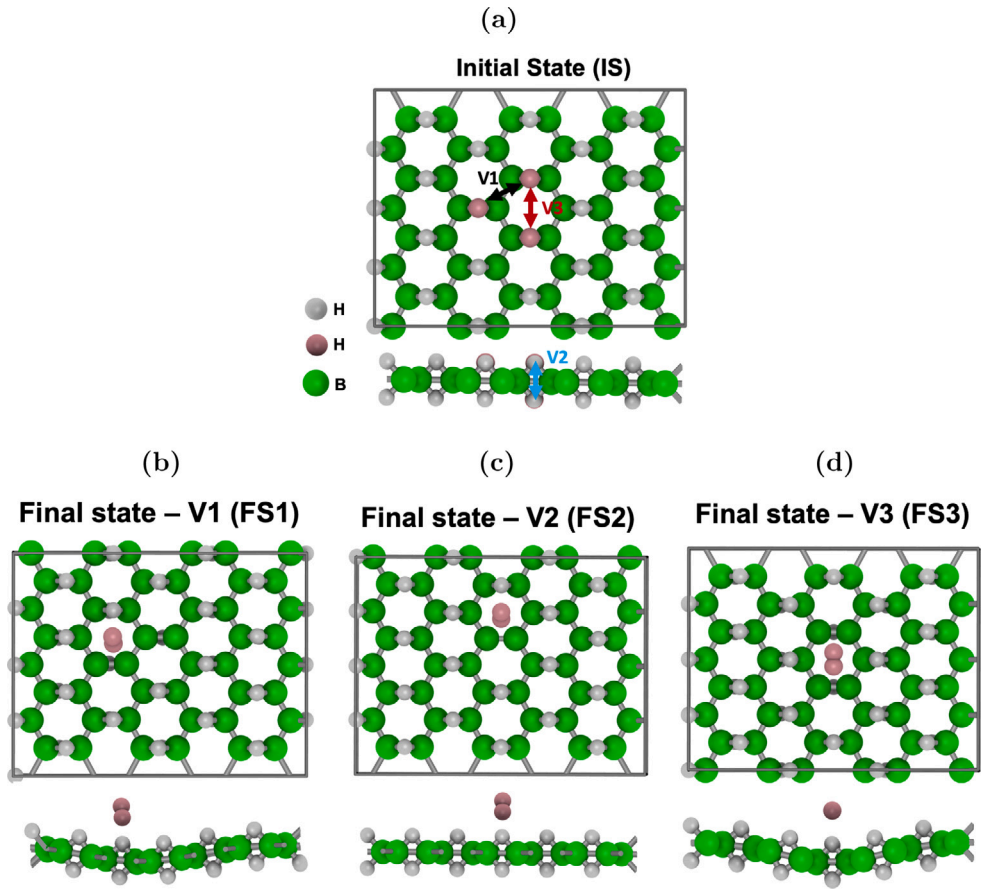

Fig. 2. Different H_2 dissociation/desorption paths on 2D BH are shown in structure (a). In the first variation (V1), two adjacent H atoms react, while in the second (V2) and third (V3) variation, two up/down and opposing H neighbors react to form H_2, respectively. The different variations, V1, V2 and V3, lead to the H_2 physisorbed states, (b), (c) and (d), respectively. The H atoms that are undergoing reaction are shown in pink while the rest of H-atoms are colored gray.

3.1.1. H_2 Desorption on Borophene-Hydride (2D BH)

The pristine structure of 2D BH stores 8.5 wt% chemisorbed H atoms [37]. To investigate the desorption of these H-atoms, different paths for H_2 formation are considered. Three different H_2 formation routes are shown in Fig. 2. To form a H_2 molecule, a H-atom can react with its adjacent (V1), and opposing (up/down (V2), and across the hollow site (V3)) neighboring H-atoms. Our DFT results indicate that the V1 reaction route (see Fig. 2(a)) is the most energetically favorable route with a heat of dehydrogenation of 1.92 eV/H_2, while the V2 and V3 formation route have a heat of dehydrogenation of 2.11, and 1.94

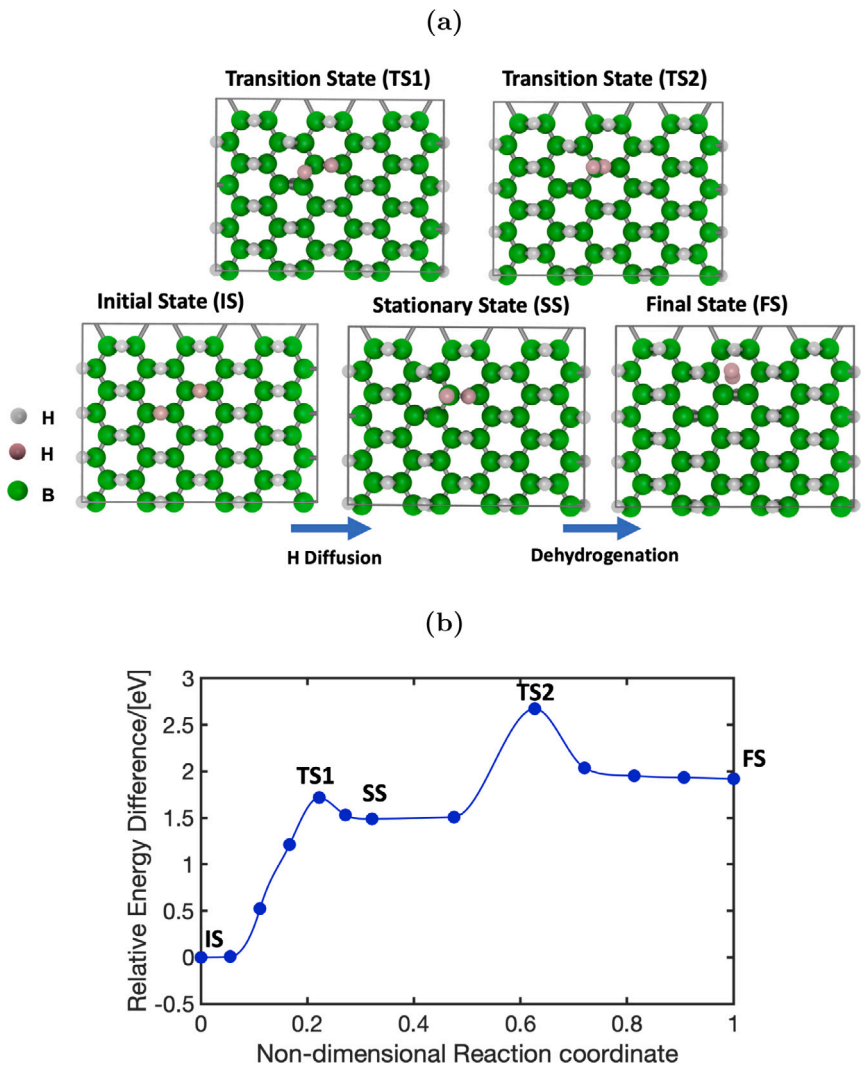

Fig. 3. (a) The structural configurations corresponding to the minimum energy pathway for a single H_2 release on 2D BH. The H atoms that are undergoing reaction are shown in pink while the rest of H-atoms are colored gray. To reach the final state from the initial state, one of the H-atoms initially hops to a neighboring boron atom (stationary state) and consequently the two H-atoms react to form a H_2 molecule. The transition states for each of the two processes are shown. (b) The minimum energy pathway for a single H_2 release for the path depicted in (a) as a function of a non-dimensional reaction coordinate. The TS1, SS, TS2, and FS states have a energy difference of 1.72, 1.53, 2.68, and 1.92 eV with respect to the IS state, respectively. The lines connecting the NEB images (constructed using forced-based cubic splines) are to guide the eye.

eV/H_2, respectively. Based on these results, it can be concluded that the physisorbed state is significantly less energetically stable than the chemisorbed state, leading to a strongly endothermic dehydrogenation reaction (ca. 2.0 eV/H_2).

In the MEP shown in Fig. 3, a two-step H_2 formation mechanism is shown for the V1 formation route (see Fig. 2(a)), with one stationary state in between the initial (chemisorbed) and final (physisorbed) states. In the first step, a H-atom initially diffuses from a bridge site towards a B atom. Subsequently, it forms an H_2 molecule by reacting with its closest neighboring H-atom. The MEP, as obtained from the NEB calculations, is shown in Fig. 3(b). For dehydrogenation to occur, two energy barriers have to be overcome, with an overall barrier (summation of the two barriers) of 2.87 eV. Other reaction pathways (with a single-step process) for dehydrogenation have also been investigated (see Figure S3 of the Supplementary Information). It is found that the two step process as shown in Fig. 3 has a 12.5% lower overall energy barrier with respect to the single step process. Overall, it can be seen that in the pristine 2D BH structure, dehydrogenation is endothermic, with large activation energy barriers. This finding shows the necessity for addition of dopants to make 2D BH suitable for H_2 chemisorption.

3.1.2. H_2 adsorption/desorption on striped-borophene

As striped borophene does not intrinsically contain any H-atoms, unlike 2D BH, a H_2 molecule is inserted to assess H_2 chemisorption. To examine the energetic stability of different possible configurations for H-atoms (for the initial chemisorbed state) and a H_2 molecule (for the final physisorbed state), three different configurations are probed for both the initial and final states. These different configurations are shown in Figure S4 of the Supplementary Information. The most energetically stable configurations are then used to calculate the H_2 chemisorption/desorption energy barrier. Fig. 4 shows the configurations and the minimum energy path of H_2 desorption or chemisorption for striped borophene. The hydrogenated state is found to be more energetically favorable than the dehydrogenated state, leading to an endothermic hydrogen release of 1.41 eV/H_2. The energy barrier for H_2 release (dehydrogenation) is 2.04 eV, which is lower than in 2D BH, but larger compared to graphene based H_2 chemisorption materials reported (usually ca. 1.5 eV [8,51]). The results obtained for the energy barrier of H_2 release on striped borophene shows adequate agreement to similar calculations reported in literature (ranging from 1.89 eV [69] to 2.21 eV [70]).

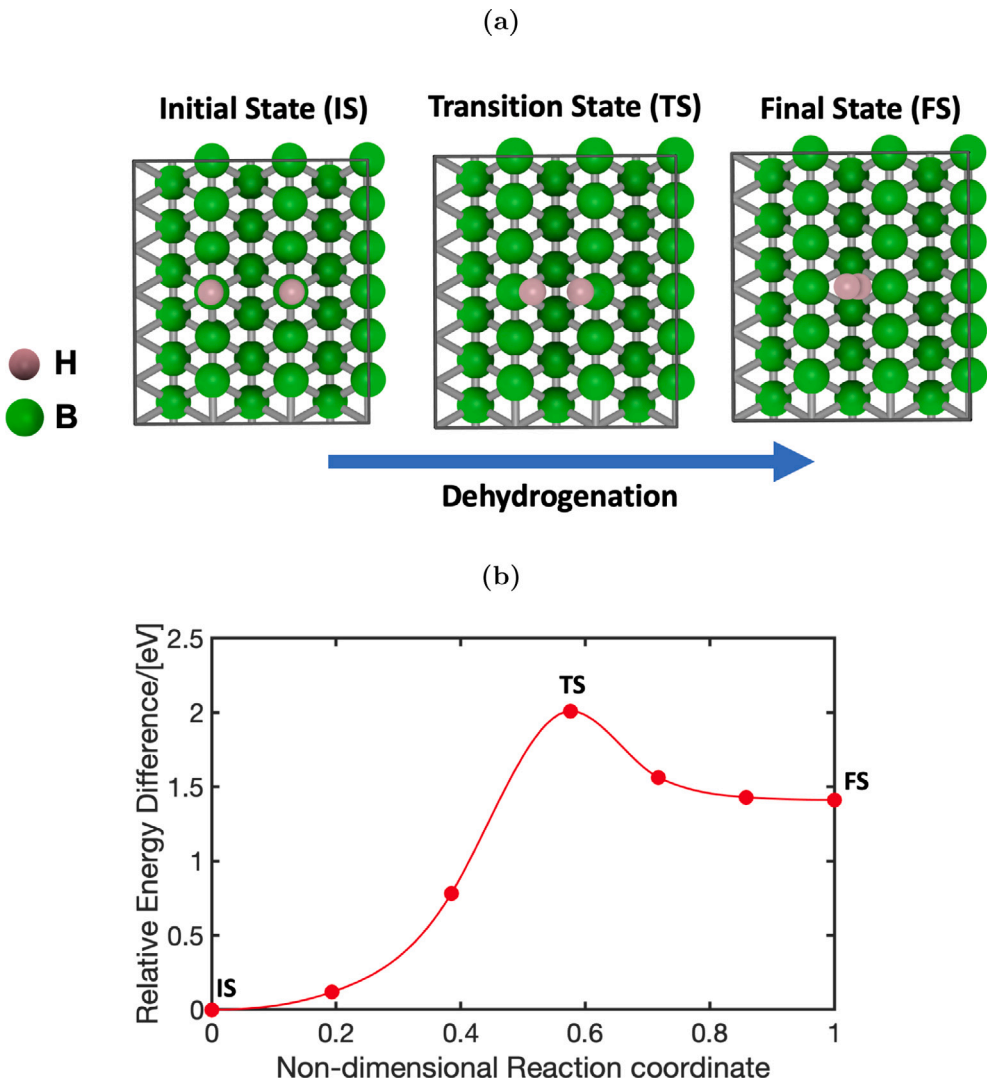

Fig. 4. (a) The minimum energy path for the release of a single H_2 on striped-borophene. The H atoms that are undergoing reaction are shown in pink. H_2 release occurs in an one-step reaction process from the chemisorbed (initial) state to the released (final) state. The transition state for the process is shown. (b) The minimum energy path for a single H_2 release for the path depicted in (a) as a function of the non-dimensional reaction coordinate. The TS, and FS states have a energy difference of 2.04, and 1.41 eV with respect to the IS state, respectively.

3.2. Doping with Li

After having established a benchmark for H_2 chemisorption and desorption on the pristine 2D structures, the influence of Li-dopants on the (de)hydrogenation reaction has been considered. To assess the stability of Li-dopants on the 2D structures, the Li-adsorption energy is calculated from [41,43]

$$E_{ads} = E_{S+nLi} - E_{S+(n-1)Li} - E_{M,C} \quad (1)$$

where E_{ads}, E_{S+nLi}, $E_{S+(n-1)Li}$, and $E_{M,C}$ are the Li adsorption energy, the energy of the substrate with n and $(n-1)$ Li atoms, and the cohesive energy of Li in its bulk metallic form, respectively. If E_{ads} is negative, then the addition of the nth Li atom is favorable. If the adsorption energy is positive, Li would rather form metal clusters than being adsorbed on the 2D substrate [43]. Based on prior findings in the literature, Li-dopants have a higher affinity for borophene-hydride compared to dopants such as Na, K, Ca and Mg [40,41]. For this reason, only Li adatoms are considered here. The study of the influence of other dopants on the dehydrogenation barriers in borophene and borophene hydride is beyond the scope of this work.

For a single Li-dopant on 2D BH, three different adsorption sites are considered, namely on top of the B or H atom, or on the vacant site. It is found that the vacant site is the most favorable position, with an adsorption energy of −0.66 eV (see Figure S5 of the Supplementary Information). Higher Li-loadings up to 4 Li-atoms are probed, and their influence on the dehydrogenation of 2D BH is investigated. As we are interested in the influence of Li-atoms on the dehydrogenation reaction shown in Fig. 3(a), the Li-atoms are placed in the proximity of the H-atoms that take part in the reaction. The different configurations of Li-doped 2D BH considered (at various Li loadings) are shown in Figure S6 in the Supplementary Information. The initial chemisorbed configuration for the 3-Li decorated 2D BH is shown in Fig. 5(a).

Table 1 shows for each of the configurations the respective Li adsorption energies, the average Bader [58] net charge state of the Li-atoms in the chemisorbed state, and the relative energy difference of the final (physisorbed) state with respect to the initial (chemisorbed) state (ΔE_{FS-IS}). The mechanism for Li charge transfer on borophene-hydride, including the electronic structure and charge density difference, is elaborated in prior studies [38,41]. The average Bader net charge state represents the net gain or loss of electronic charge density of an atom [58] due to its environment, and shows the degree of charge density loss by the Li-dopant onto the 2D substrate at various Li-loadings. Our results indicate that the addition of Li-dopants increases the energetic stability of the final state (physisorbed) with respect to the

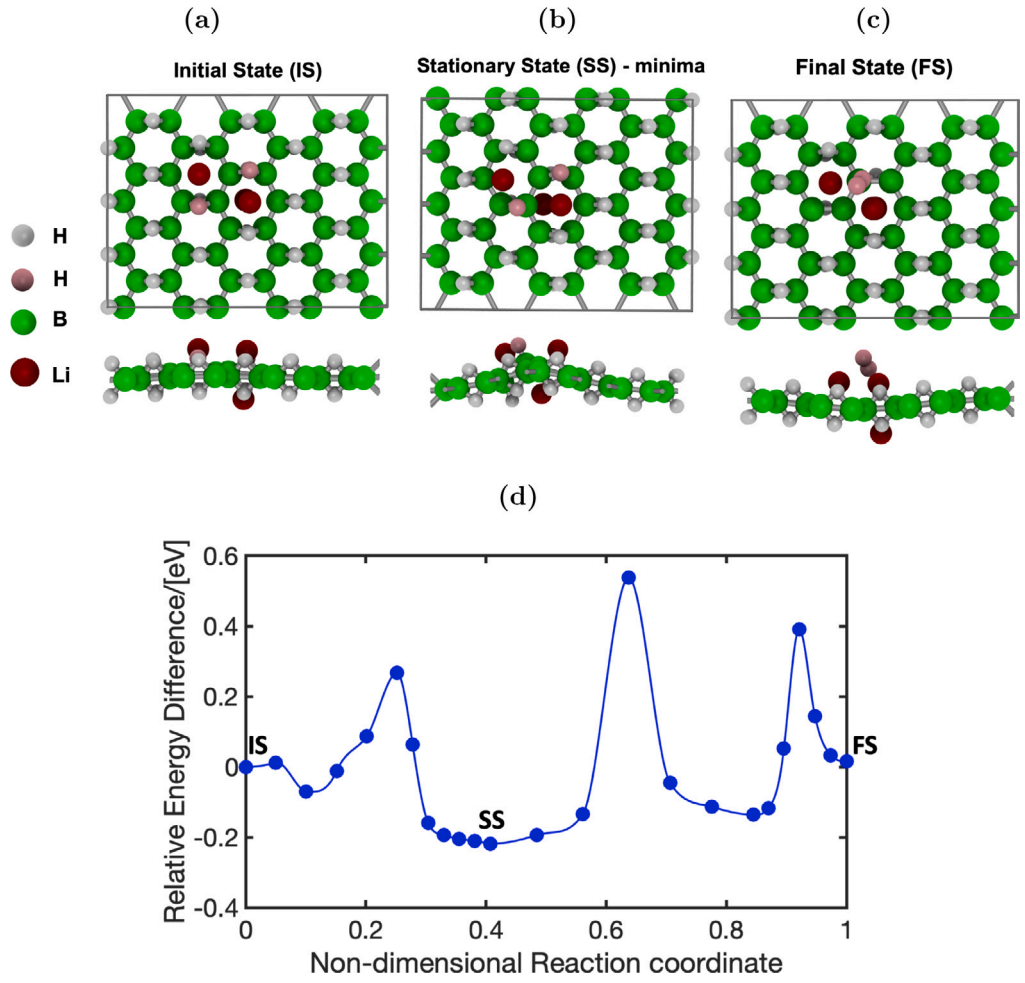

Fig. 5. Top and side views of the (a) initial state, (b) most stable stationary state (minima), and (c) final state of 3Li-2D BH. The H atoms that are undergoing reaction are shown in pink while the rest of H-atoms are colored gray. (d) The minimum energy path for a single H_2 dehydrogenation on 3Li-2D BH. The relative energy with respect to the initial state is shown as a function of the non-dimensional reaction coordinate. The SS, and FS states have a energy difference of −0.22, and 0.02 eV with respect to the IS state, respectively.

Table 1
The Li-adsorption energy ($E_{ads,Li}$), and the average Li-Bader net charge state on 2D BH at different loadings of Li. For the Bader net charge state, the plus sign indicates a gain of electronic charge density and a minus sign indicates a loss of electronic charge density with respect to the atomic charge of respective elements (net charge 0). The energy difference between the final (physisorbed) and initial (chemisorbed) state (ΔE_{FS-IS}) is shown at different Li-doped configuration (see Figure S6 of the Supplementary Information for the structures).

Configuration	$E_{ads,Li}$ [eV]	Avg Li Bader net charge [e]	ΔE_{FS-IS} [eV]
2D BH	–	–	1.94
Li-2D BH	−0.66	−0.88	1.11
2Li-2D BH	−0.53	−0.87	0.58
3Li-2D BH	−0.45	−0.87	0.02
4Li-2D BH	−0.30	−0.87	−0.50

initial state (chemisorbed), leading to a transition from endothermic to exothermic dehydrogenation on 2D BH. Specifically for the structures shown in Fig. 5(a) and (c) (3Li-2D BH configuration), the initial and final state are close in energy, thereby making dehydrogenation a much more reversible reaction when compared to the pristine case.

The minimum energy path for the dehydrogenation reaction on the 3Li-2D BH configuration is shown in Fig. 5(d) as a function of the non-dimensional reaction coordinate. The full schematic of this minimum energy path, including all the stationary and transition states, is shown in Figure S7 in the Supplementary Information. In the case of pristine 2D BH, 3 center 2 electron bonds (B-H-B) provided the most stable state along the reaction path way (see Fig. 3(b)), but in the presence of few Li-dopants, the state with the minimum energy is a stationary state in which two B-H bonds have replaced two B-H-B bonds. This may be due to the charge donating nature of Li-atoms (as shown by the negative Bader net charges in Table 1), which weakens the electron deficient 3-center-2 electron bonds present in B-H-B. This result is supported by our BOMD simulations at 300 K (simulation snapshots are shown in Fig. 6), which show that upon addition of Li, the H atoms in the vicinity of Li-atoms can escape the bridge site of B-atoms, while in the pristine case, H-atoms only exhibit vibrations around the bridge site. By subtracting the energy of the final H_2 physisorbed state (see Fig. 5(c)) from the most stable stationary state (see Fig. 5(b)), a heat of reaction (dehydrogenation) of 0.24 eV/H_2 can be obtained. This heat of dehydrogenation is 88% lower than for pristine 2D BH (i.e., 1.92 eV/H_2).

Based on the results of Fig. 5, it can be concluded that the energy barriers for dehydrogenation have reduced significantly in the presence of Li-atoms. The magnitude of the largest activation barrier for the dehydrogenation reaction (ca. 0.8 eV) is significantly lower than the activation energy for the pristine case (i.e., 2.86 eV), and the number of stationary states present along the reaction pathway has considerably increased in the presence of Li-dopants. Excluding the initial and final state, there are 3 stationary states along the reaction pathway for 3Li-2D BH compared to 1 in the pristine case. This can be attributed to the more complex potential energy landscape that forms due to the addition of Li.

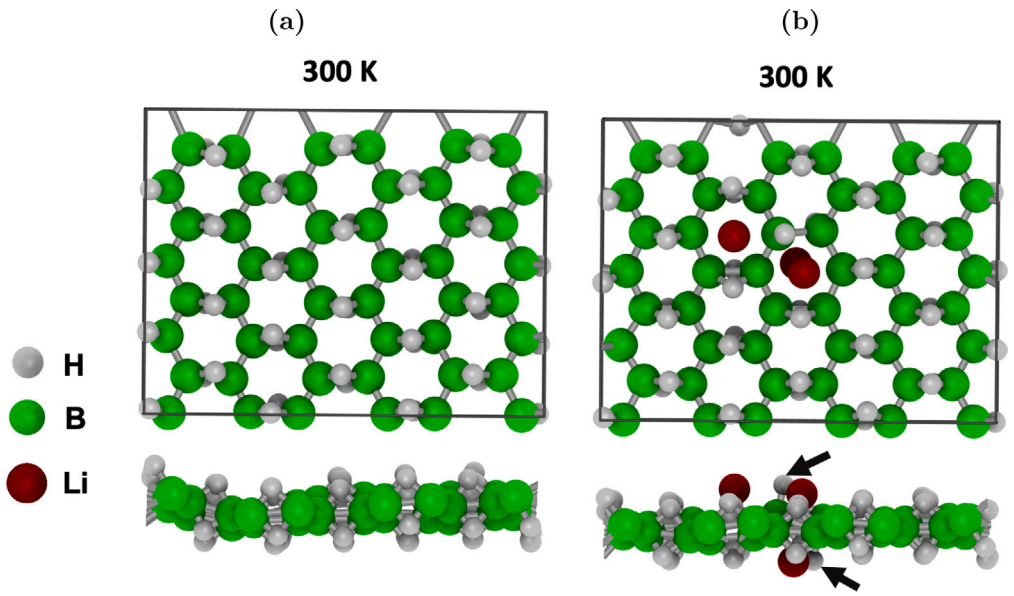

Fig. 6. Top and side views of BOMD simulation snapshots after a 12 ps run at 300 K for (a) borophene-hydride, (b) 3Li-doped borophene-hydride. For borophene-hydride, the H-atoms exhibit vibrations around the bridge site of the boron atoms (3-center-2 electron bonds). In the 3Li-2D BH configuration two H-atoms (indicated by the black arrows) escape the bridge bond (one at the top and one at the bottom of the layer).

Overall, it can be seen that Li-dopants can have a significant influence on both the energy barriers and favorability of the dehydrogenation reaction on 2D BH. This means that for applications that require large loadings of Li on 2D BH, such as for Li anode batteries, and physisorptive storage of H_2 by means of Li dopants, both the reconfiguration of the B-H-B bond and the possibility for dehydrogenation needs to be considered. Our results further entail that by tuning the Li-loading it may be possible to release the chemisorbed H-atoms in a reversible manner with enhanced adsorption/desorption kinetics (lower energy barriers).

Similarly for the case of striped-borophene, Li-dopants are added to examine their influence on H_2 chemisorption and dehydrogenation. The Li-atoms are positioned in the proximity of (to the sides and below) the H-atom adsorption sites (shown in Fig. 7(a) for the 3-Li doped striped borophene configuration). All different Li configurations that are probed are shown in Figure S8 in the Supplementary Information. Table 2 shows the Li adsorption energies, the average Bader net charge state of Li, and the energetic difference between the final (physisorbed) and initial (chemisorbed) state (ΔE_{FS-IS}). The mechanism for Li charge transfer on striped-borophene is elaborated in prior studies [71,72].

In striped-borophene, Li-dopants have reduced the energy difference between the chemisorbed (hydrogenated) and physisorbed state by ca. 50% compared to the pristine striped-borophene (1.41 eV). Based on the minimum energy path shown in Fig. 7(d), it can be seen that the dehydrogenation barriers have been reduced by ca. 30% (1.34 eV) with respect to the dehydrogenation barrier of the pristine case (2.04 eV based on Fig. 3). The full schematic of this minimum energy path, including all the stationary and transition states is shown in Figure S10 in the Supplementary Information. The reason why in 2D BH, the influence of Li-dopants on the endothermicity of dehydrogenation is larger than in striped borophene, may be due to the different bonding type of H-atoms in the two structures. Overall, it can be seen that Li-dopants have a significant effect on the chemisorption and dehydrogenation properties of striped-borophene as well. Further study is needed to optimize the dopant loadings and to observe these effects experimentally. In a realistic H_2 storage material, the 2D layers have to be stacked on each other forming a layered 3D structure. The calculation of the optimum layering distance, gravimetric or volumetric capacity of H_2 in these materials is beyond the scope of our work.

Table 2
The Li-adsorption energy ($E_{ads,Li}$), and the average Li-Bader net charge state on striped borophene at different loadings of Li. For the Bader net charge state, the plus sign indicates a gain of electronic charge density and a minus sign indicates a loss of electronic charge density with respect to the atomic charge of respective elements (net charge 0). The energy difference between the final (physisorbed) and initial (chemisorbed) state (ΔE_{FS-IS}) is shown at different Li-doped configurations (see Figure S9 of the Supplementary Information for the structures).

Configuration	$E_{ads,Li}$ [eV]	Avg Li Bader net charge [e]	ΔE_{FS-IS} [eV]
B Striped	–	–	1.41
Li-B striped	−1.54	−0.89	1.02
2Li-B striped	−1.12	−0.89	0.83
3Li-B striped	−1.56	−0.88	0.73
4Li-B striped	−1.32	−0.88	0.84

4. Conclusions

The influence of Li-dopants at various loadings on H_2 chemisorption and desorption barriers of borophene-hydride and striped-borophene are assessed using first-principle calculations. In the pristine case, it is found that dehydrogenation of borophene-hydride and striped-borophene is highly endothermic. The energy barriers for H_2 desorption are also large (2.04 eV for striped-borophene and 2.87 eV for borophene-hydride). Both of these factors limit the application of this material for H_2 chemisorption applications. With the addition of Li, the relative energy difference between the chemisorbed and physisorbed states is significantly decreased. In 3-Li doped borophene-hydride and striped borophene, there is ca. 90% and 50% decrease in the endothermicity of the dehydrogenation reaction, respectively, with respect to the pristine 2D structures. The BOMD simulations for 2D BH at 300 K show that the 3-center-2-electron bond weakens in the presence of Li dopants. The dehydrogenation barriers are also reduced by more than 30% for both structures in the presence of Li-dopants. Our findings show that Li-dopants (especially at high loadings) strongly influence the hydrogenation/dehydrogenation reaction of borophene-hydride and striped borophene, and may encourage experimental studies on Li-doped borophene-hydride as a potential H_2 chemisorptive storage medium.

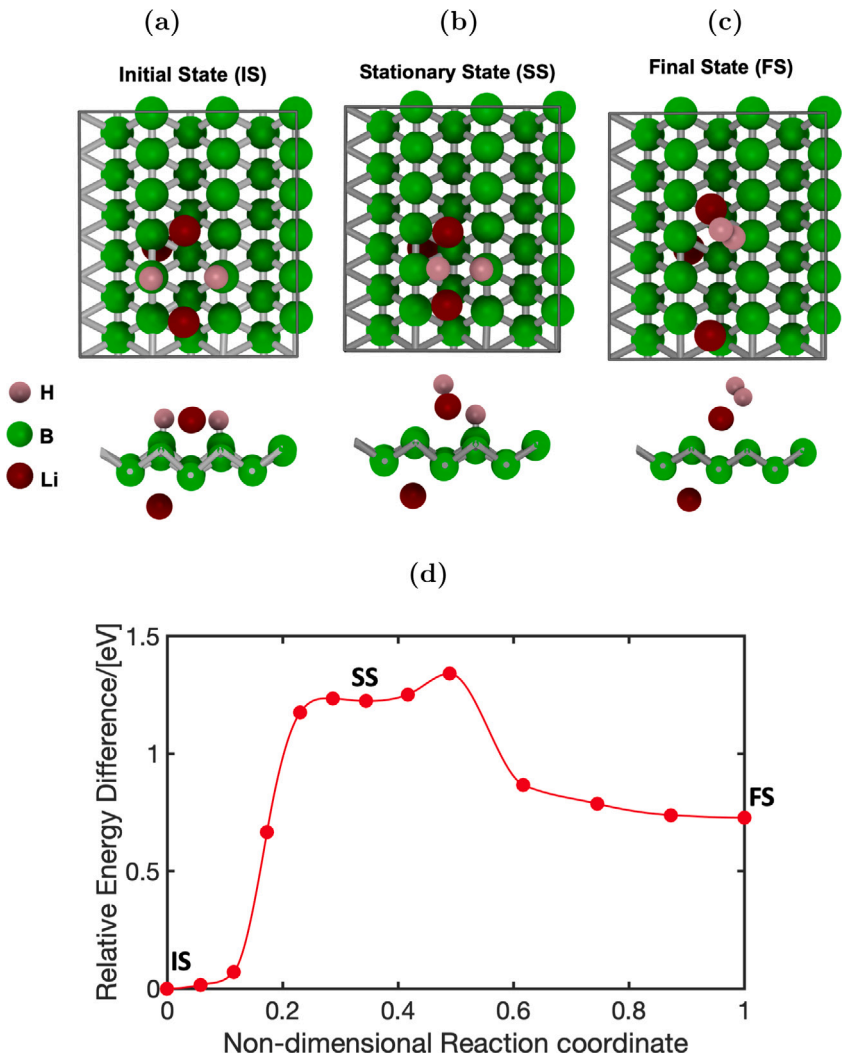

Fig. 7. Top and side views of the (a) initial state, (b) stationary state, and (c) final state of 3 Li doped striped borophene. The H atoms that are undergoing reaction are shown in pink. (d) The minimum energy path for single H_2 dehydrogenation on 3-Li doped striped borophene. The relative energy with respect to the initial state is shown as a function of the non-dimensional reaction coordinate for the dehydrogenation reaction. The SS, and FS states have a energy difference of 1.22, and 0.73 eV with respect to the IS state, respectively.

CRediT authorship contribution statement

Parsa Habibi: Conceptualization, Methodology, Investigation, Writing – original draft. **Tijin H.G. Saji:** Methodology, Investigation, Writing – review & editing. **Thijs J.H. Vlugt:** Conceptualization, Methodology, Writing – review & editing, Supervision. **Othonas A. Moultos:** Conceptualization, Methodology, Writing – review & editing, Supervision. **Poulumi Dey:** Conceptualization, Methodology, Writing – review & editing, Supervision.

Declaration of competing interest

The authors declare that they have no known competing financial interests or personal relationships that could have appeared to influence the work reported in this paper.

Data availability

Data will be made available on request.

Acknowledgments

This work was sponsored by NWO Domain Science for the use of supercomputer facilities. Thijs J.H. Vlugt acknowledges NWO-CW for a VICI grant.

Appendix A. Supplementary information

Comparison of heat of dehydrogenation results obtained from DFT-D2 and DFT-D3 for pristine and 3-Li doped borophene hydride and striped borophene; System size choice for borophene hydride and striped borophene; Convergence study for the number of K-points, Free energy and temperature plots as a function of time during Born–Oppenheimer Molecular dynamics simulations of 2D BH (with and without Li dopant); Different H_2 release paths on 2D BH; Different initial (chemisorbed) and final (physisorbed) H_2 configurations on striped-borophene; Different single Li adsorption sites on 2D BH; Different configurations of Li doped 2D BH at different (2, 3 and 4-Li) loadings; Minimum energy path for H_2 release on 3-Li doped 2D BH showing all stationary and transition states; Different single Li adsorption sites on striped borophene; Different configurations of Li doped striped borophene at different (2, 3 and 4-Li) loadings; Minimum

energy path for H_2 release on 3-Li doped striped borophene showing all stationary and transition states.

Supplementary material related to this article can be found online at https://doi.org/10.1016/j.apsusc.2022.154323.

References

[1] A. Züttel, Materials for hydrogen storage, Mater. Today 6 (9) (2003) 24–33, 10.1016/S1369-7021(03)00922-2.

[2] S. Kumar, T.J. Dhilip Kumar, Electronic structure calculations of hydrogen storage in lithium-decorated metal-graphyne framework, ACS Appl. Mater. Interfaces 9 (34) (2017) 28659–28666.

[3] P. Jena, Materials for hydrogen storage: Past, present, and future, J. Phys. Chem. Lett. 2 (3) (2011) 206–211.

[4] D. Durbin, C. Malardier-Jugroot, Review of hydrogen storage techniques for on board vehicle applications, Int. J. Hydrogen Energy 38 (34) (2013) 14595–14617.

[5] U. Eberle, M. Felderhoff, F. Schueth, Chemical and physical solutions for hydrogen storage, Angew. Chem., Int. Ed. Engl. 48 (36) (2009) 6608–6630.

[6] J. Ren, N.M. Musyoka, H.W. Langmi, M. Mathe, S. Liao, Current research trends and perspectives on materials-based hydrogen storage solutions: A critical review, Int. J. Hydrogen Energy 42 (1) (2017) 289–311.

[7] A. Schneemann, J.L. White, S. Kang, S. Jeong, L.F. Wan, E.S. Cho, T.W. Heo, D. Prendergast, J.J. Urban, B.C. Wood, M.D. Allendorf, V. Stavila, Nanostructured metal hydrides for hydrogen storage, Chem. Rev. 118 (22) (2018) 10775–10839.

[8] G.K. Sunnardianto, G. Bokas, A. Hussein, C. Walters, O.A. Moultos, P. Dey, Efficient hydrogen storage in defective graphene and its mechanical stability: A combined density functional theory and molecular dynamics simulation study, Int. J. Hydrogen Energy 46 (7) (2021) 5485–5494.

[9] S. Er, G.A. de Wijs, G. Brocks, Tuning the hydrogen storage in magnesium alloys, J. Phys. Chem. Lett. 1 (13) (2010) 1982–1986.

[10] L. Zang, W. Sun, S. Liu, Y. Huang, H. Yuan, Z. Tao, Y. Wang, Enhanced hydrogen storage properties and reversibility of $LiBH_4$ confined in two-dimensional Ti_3C_2, ACS Appl. Mater. Interfaces 10 (23) (2018) 19598–19604.

[11] G. Liu, Y. Wang, L. Jiao, H. Yuan, Understanding the role of few-layer graphene nanosheets in enhancing the hydrogen sorption kinetics of magnesium hydride, ACS Appl. Mater. Interfaces 6 (14) (2014) 11038–11046.

[12] A. Yadav, A. Dashora, N. Patel, A. Miotello, M. Press, D. Kothari, Study of 2D MXene Cr2C material for hydrogen storage using density functional theory, Appl. Surf. Sci. 389 (2016) 88–95.

[13] J. Zhang, T.S. Fisher, P.V. Ramachandran, J.P. Gore, I. Mudawar, A review of heat transfer issues in hydrogen storage technologies, J. Heat Transfer 127 (12) (2005) 1391–1399.

[14] M. Felderhoff, C. Weidenthaler, R. von Helmolt, U. Eberle, Hydrogen storage: the remaining scientific and technological challenges, Phys. Chem. Chem. Phys. 9 (21) (2007) 2643–2653.

[15] M. Visaria, I. Mudawar, T. Pourpoint, S. Kumar, Study of heat transfer and kinetics parameters influencing the design of heat exchangers for hydrogen storage in high-pressure metal hydrides, Int. J. Heat Mass Transfer 53 (9) (2010) 2229–2239.

[16] P. Habibi, T.J.H. Vlugt, P. Dey, O.A. Moultos, Reversible hydrogen storage in metal-decorated honeycomb borophene oxide, ACS Appl. Mater. Interfaces 13 (36) (2021) 43233–43240.

[17] A. Hashmi, M.U. Farooq, I. Khan, J. Son, J. Hong, Ultra-high capacity hydrogen storage in a Li decorated two-dimensional C_2N layer, J. Mater. Chem. A 5 (6) (2017) 2821–2828.

[18] X. Liang, S.-P. Ng, N. Ding, C.-M.L. Wu, Strain-induced switch for hydrogen storage in cobalt-decorated nitrogen-doped graphene, Appl. Surf. Sci. 473 (2019) 174–181.

[19] D. Kag, N. Luhadiya, N.D. Patil, S. Kundalwal, Strain and defect engineering of graphene for hydrogen storage via atomistic modelling, Int. J. Hydrogen Energy 46 (43) (2021) 22599–22610.

[20] V. Surya, K. Iyakutti, H. Mizuseki, Y. Kawazoe, Modification of graphene as active hydrogen storage medium by strain engineering, Comput. Mater. Sci. 65 (2012) 144–148.

[21] L. Li, H. Zhang, X. Cheng, The high hydrogen storage capacities of Li-decorated borophene, Comput. Mater. Sci. 137 (2017) 119–124.

[22] Y. Wang, G. Xu, S. Deng, Q. Wu, Z. Meng, X. Huang, L. Bi, Z. Yang, R. Lu, Lithium and sodium decorated graphdiyne as a candidate for hydrogen storage: First-principles and grand canonical Monte Carlo study, Appl. Surf. Sci. 509 (2020) 144855.

[23] T. Liu, Y. Chen, H. Wang, M. Zhang, L. Yuan, C. Zhang, Li-decorated β_{12}-borophene as potential candidates for hydrogen storage: A first-principle study, Materials 10 (12) (2017).

[24] Y. Zhang, L. Zhang, H. Pan, H. Wang, Q. Li, Li-decorated porous hydrogen substituted graphyne: A new member of promising hydrogen storage medium, Appl. Surf. Sci. 535 (2021) 147683.

[25] D. John, B. Nharangatt, S. Madhav Kastuar, R. Chatanathodi, Blue phosphorene nanosheets with point defects: Electronic structure and hydrogen storage capability, Appl. Surf. Sci. 551 (2021) 149363.

[26] X. Tan, H.A. Tahini, S.C. Smith, Conductive boron-doped graphene as an ideal material for electrocatalytically switchable and high-capacity hydrogen storage, ACS Appl. Mater. Interfaces 8 (48) (2016) 32815–32822.

[27] X. Li, X. Tan, Q. Xue, S. Smith, Charge-controlled switchable H_2 storage on conductive borophene nanosheet, Int. J. Hydrogen Energy 44 (36) (2019) 20150–20157.

[28] S. Goler, C. Coletti, V. Tozzini, V. Piazza, T. Mashoff, F. Beltram, V. Pellegrini, S. Heun, Influence of graphene curvature on hydrogen adsorption: Toward hydrogen storage devices, J. Phys. Chem. C 117 (22) (2013) 11506–11513.

[29] V. Tozzini, V. Pellegrini, Reversible hydrogen storage by controlled buckling of graphene layers, J. Phys. Chem. C 115 (51) (2011) 25523–25528.

[30] A.J. Mannix, X.-F. Zhou, B. Kiraly, J.D. Wood, D. Alducin, B.D. Myers, X. Liu, B.L. Fisher, U. Santiago, J.R. Guest, M.J. Yacaman, A. Ponce, A.R. Oganov, M.C. Hersam, N.P. Guisinger, Synthesis of borophenes: Anisotropic, two-dimensional boron polymorphs, Science 350 (6267) (2015) 1513–1516.

[31] W. Li, L. Kong, C. Chen, J. Gou, S. Sheng, W. Zhang, H. Li, L. Chen, P. Cheng, K. Wu, Experimental realization of honeycomb borophene, Sci. Bull. 63 (5) (2018) 282–286.

[32] B. Kiraly, X. Liu, L. Wang, Z. Zhang, A.J. Mannix, B.L. Fisher, B.I. Yakobson, M.C. Hersam, N.P. Guisinger, Borophene synthesis on Au(111), ACS Nano 13 (4) (2019) 3816–3822, PMID: 30844248.

[33] Y. Wang, Y. Park, L. Qiu, I. Mitchell, F. Ding, Borophene with large holes, J. Phys. Chem. Lett. 11 (15) (2020) 6235–6241.

[34] S. Er, G.A. de Wijs, G. Brocks, DFT study of planar boron sheets: A new template for hydrogen storage, J. Phys. Chem. C 113 (43) (2009) 18962–18967.

[35] Y. Liu, V.I. Artyukhov, M. Liu, A.R. Harutyunyan, B.I. Yakobson, Feasibility of lithium storage on graphene and its derivatives, J. Phys. Chem. Lett. 4 (10) (2013) 1737–1742.

[36] H. Nishino, T. Fujita, A. Yamamoto, T. Fujimori, A. Fujino, S.-i. Ito, J. Nakamura, H. Hosono, T. Kondo, Formation mechanism of boron-based nanosheet through the reaction of MgB2 with water, J. Phys. Chem. C 121 (19) (2017) 10587–10593.

[37] R. Kawamura, N.T. Cuong, T. Fujita, R. Ishibiki, T. Hirabayashi, A. Yamaguchi, I. Matsuda, S. Okada, T. Kondo, M. Miyauchi, Photoinduced hydrogen release from hydrogen boride sheets, Nature Commun. 10 (1) (2019) 25523–25528.

[38] M. Makaremi, B. Mortazavi, C.V. Singh, 2D hydrogenated graphene-like borophene as a high capacity anode material for improved Li/Na ion batteries: A first principles study, Mater. Today Energy 8 (2018) 22–28.

[39] Y. Jiao, F. Ma, J. Bell, A. Bilic, A. Du, Two-dimensional boron hydride sheets: High stability, massless Dirac Fermions, and excellent mechanical properties, Angew. Chem., Int. Ed. Engl. 128 (35) (2016) 10448–10451.

[40] V. Shukla, R.B. Araujo, N.K. Jena, R. Ahuja, Borophene's tryst with stability: Exploring 2D hydrogen boride as an electrode for rechargeable batteries, Phys. Chem. Chem. Phys. 20 (34) (2018) 22008–22016.

[41] L. Chen, X. Chen, C. Duan, Y. Huang, Q. Zhang, B. Xiao, Reversible hydrogen storage in pristine and Li decorated 2D boron hydride, Phys. Chem. Chem. Phys. 20 (48) (2018) 30304–30311.

[42] N. Khossossi, Y. Benhouria, S.R. Naqvi, P.K. Panda, I. Essaoudi, A. Ainane, R. Ahuja, Hydrogen storage characteristics of Li and Na decorated 2D boron phosphide, Sustain. Energy Fuels 4 (9) (2020) 4538–4546.

[43] S. Haldar, S. Mukherjee, C.V. Singh, Hydrogen storage in Li, Na and Ca decorated and defective borophene: a first principles study, RSC Adv. 8 (37) (2018) 20748–20757.

[44] I. Cabria, A. Lebon, M. Torres, L. Gallego, A. Vega, Hydrogen storage capacity of li-decorated borophene and pristine graphene slit pores: A combined ab initio and quantum-thermodynamic study, Appl. Surf. Sci. 562 (2021) 150019.

[45] B. Peng, H. Zhang, H. Shao, Z. Ning, Y. Xu, G. Ni, H. Lu, D.W. Zhang, H. Zhu, Stability and strength of atomically thin borophene from first principles calculations, Mater. Res. Lett. 5 (6) (2017) 399–407.

[46] B. Mortazavi, M. Makaremi, M. Shahrokhi, M. Raeisi, C.V. Singh, T. Rabczuk, L.F.C. Pereira, Borophene hydride: a stiff 2D material with high thermal conductivity and attractive optical and electronic properties, Nanoscale 10 (8) (2018) 3759–3768.

[47] Z.-Q. Wang, T.-Y. Lü, H.-Q. Wang, Y.P. Feng, J.-C. Zheng, Review of borophene and its potential applications, Front. Phys. 14 (3) (2019) 1–20.

[48] T.A. Abtew, P. Zhang, Charging-assisted hydrogen release mechanism in layered boron hydride, Phys. Rev. B 84 (2011) 094303.

[49] T.A. Abtew, B.-c. Shih, P. Dev, V.H. Crespi, P. Zhang, Prediction of a multicenter-bonded solid boron hydride for hydrogen storage, Phys. Rev. B 83 (2011) 094108.

[50] N.K. Jena, R.B. Araujo, V. Shukla, R. Ahuja, Borophane as a benchmate of graphene: A potential 2D material for anode of Li and Na-Ion batteries, ACS Appl. Mater. Interfaces 9 (19) (2017) 16148–16158.

[51] V. Tozzini, V. Pellegrini, Prospects for hydrogen storage in graphene, Phys. Chem. Chem. Phys. 15 (1) (2013) 80–89.

[52] G. Kresse, J. Furthmüller, Efficiency of ab-initio total energy calculations for metals and semiconductors using a plane-wave basis set, Comput. Mater. Sci. 6 (1) (1996) 15–50.

[53] G. Kresse, J. Furthmüller, Efficient iterative schemes for ab-initio total-energy calculations using a plane-wave basis set, Phys. Rev. B 54 (1996) 11169–11186.

[54] J.P. Perdew, K. Burke, M. Ernzerhof, Generalized gradient approximation made simple, Phys. Rev. Lett. 77 (18) (1996) 3865.
[55] S. Grimme, Semiempirical GGA-type density functional constructed with a long-range dispersion correction, J. Comput. Chem. 27 (15) (2006) 1787–1799.
[56] T. Wen, A. Xie, J. Li, Y. Yang, Novel ti-decorated borophene $\chi 3$ as potential high-performance for hydrogen storage medium, Int. J. Hydrogen Energy 45 (53) (2020) 29059–29069.
[57] S. Grimme, J. Antony, S. Ehrlich, H. Krieg, A consistent and accurate ab initio parametrization of density functional dispersion correction (DFT-D) for the 94 elements H-Pu, J. Chem. Phys. 132 (15) (2010) 154104.
[58] G. Henkelman, A. Arnaldsson, H. Jónsson, A fast and robust algorithm for bader decomposition of charge density, Comput. Mater. Sci. 36 (3) (2006) 354–360.
[59] W. Tang, E. Sanville, G. Henkelman, A grid-based bader analysis algorithm without lattice bias, J. Phys.: Condens. Matter 21 (8) (2009) 084204.
[60] E. Sanville, S.D. Kenny, R. Smith, G. Henkelman, Improved grid-based algorithm for bader charge allocation, J. Comput. Chem. 28 (5) (2007) 899–908.
[61] M. Yu, D.R. Trinkle, Accurate and efficient algorithm for Bader charge integration, J. Chem. Phys. 134 (6) (2011) 064111.
[62] G. Henkelman, H. Jónsson, Improved tangent estimate in the nudged elastic band method for finding minimum energy paths and saddle points, J. Chem. Phys. 113 (22) (2000) 9978–9985.
[63] D. Sheppard, R. Terrell, G. Henkelman, Optimization methods for finding minimum energy paths, J. Chem. Phys. 128 (13) (2008) 134106.
[64] G. Henkelman, B.P. Uberuaga, H. Jónsson, A climbing image nudged elastic band method for finding saddle points and minimum energy paths, J. Chem. Phys. 113 (22) (2000) 9901–9904.
[65] S. Nosé, A unified formulation of the constant temperature molecular dynamics methods, J. Chem. Phys. 81 (1) (1984) 511–519.
[66] W.G. Hoover, Canonical dynamics: Equilibrium phase-space distributions, Phys. Rev. A 31 (3) (1985) 1695.
[67] L. Verlet, Computer “experiments” on classical fluids. I. Thermodynamical properties of lennard-jones molecules, Phys. Rev. 159 (1967) 98–103.
[68] D. Dubbeldam, S. Calero, T.J.H. Vlugt, iRASPA: GPU-accelerated visualization software for materials scientists, Mol. Simul. 44 (8) (2018) 653–676.
[69] X. Chen, J. Liu, W. Zhang, B. Xiao, P. Zhang, L. Li, First-principles study on the mechanism of hydrogen decomposition and spillover on borophene, J. Phys. Chem. C 121 (32) (2017) 17314–17320.
[70] G. Qin, A. Du, Q. Sun, A theoretical insight into a feasible strategy for the fabrication of borophane, Phys. Chem. Chem. Phys. 20 (23) (2018) 16216–16221.
[71] L. Wang, X. Chen, H. Du, Y. Yuan, H. Qu, M. Zou, First-principles investigation on hydrogen storage performance of Li, Na and K decorated borophene, Appl. Surf. Sci. 427 (2018) 1030–1037.
[72] P. Liang, Y. Cao, B. Tai, L. Zhang, H. Shu, F. Li, D. Chao, X. Du, Is borophene a suitable anode material for sodium ion battery? J. Alloys Compd. 704 (2017) 152–159.